

Decoding of human hand actions to handle missing limbs in Neuroprosthetics

Jovana J. Belić^{1,2,3*}, Aldo A. Faisal^{1,4,5}

¹ Department of Bioengineering, Imperial College London, London, UK

² Faculty of Electrical Engineering, University of Belgrade, Belgrade, Serbia

³ Department of Computational Biology, Royal Institute of Technology KTH, Stockholm, Sweden

⁴ Department of Computing, Imperial College London, London, UK

⁵ MRC Clinical Sciences Center, London, UK

* **Correspondence:** Jovana J. Belić, Royal Institute of Technology KTH, Department of Computational Biology, 100 44 Stockholm, Sweden.
belic@kth.se

Keywords: Neurotechnology, motor control, prosthetic hand, neuroprosthetics, movement variability, Bayesian classifier, PPCA, activities of daily living, finger movement.

Abstract

The only way we can interact with the world is through movements, and our primary interactions are via the hands, thus any loss of hand function has immediate impact on our quality of life. However, to date it has not been systematically assessed how coordination in the hand's joints affects every day actions. This is important for two fundamental reasons. Firstly, to understand the representations and computations underlying motor control “in-the-wild” situations, and secondly to develop smarter controllers for prosthetic hands that have the same functionality as natural limbs. In this work we exploit the correlation structure of our hand and finger movements in daily-life. The novelty of our idea is that instead of averaging variability out, we take the view that the structure of variability may contain valuable information about the task being performed. We asked seven subjects to interact in 17 daily-life situations, and quantified behaviour in a principled manner using CyberGlove body sensor networks that, after accurate calibration, track all major joints of the hand. Our key findings are: 1. We confirmed that hand control in daily-life tasks is very low-dimensional, with four to five dimensions being sufficient to explain 80-90% of the variability in the natural movement data. 2. We established a universally applicable measure of manipulative complexity that allowed us to measure and compare limb movements across tasks. We used Bayesian latent variable models to model the low-dimensional structure of finger joint angles in natural actions. 3. This allowed us to build a naïve classifier that within the first 1000ms of action initiation (from a flat hand start configuration) predicted which of the 17 actions was going to be executed - enabling us to reliably predict the action intention from very short-time-scale initial data, further revealing the foreseeable nature of hand movements for control of neuroprosthetics and tele operation purposes. 4. Using the Expectation-Maximization algorithm on our latent variable model permitted us to reconstruct with high accuracy (<5°-6° MAE) the movement trajectory of missing fingers by simply tracking the remaining fingers. Overall, our results suggest the hypothesis that specific hand actions are orchestrated by the brain in such a way that in the natural tasks of daily-life there is sufficient redundancy and predictability to be directly exploitable for neuroprosthetics.

42

43 1. Introduction

44 The human hand is a highly complex actuator and perhaps the most important and diverse tool we
45 use to interact with the environment. The hand is capable of both a powerful grip to push, pull, or
46 twist objects, and a precise grip to twist and turn small objects or handles (Napier, 1980). These are
47 just a few of the countless gestures we can use and learn. Anatomically, the hand comprises a total of
48 27 bones, 18 joints, and 39 muscles (Tubiana, 1981), which afford over 20 degrees of freedom (DOF)
49 (Stockwell, 1981; Soechting and Flanders, 1997; Jones and Lederman, 2006). The number of degrees
50 of freedom is an important characterization of the human hand because it defines the dimensionality
51 of the control problem that has to be solved by the motor system. However, previous studies of
52 human motor control showed that normal hand behaviour uses only a small subset of possible hand
53 configurations (Todorov and Ghahramani, 2004; Weiss and Flanders, 2004; Ingram et al., 2008;
54 Valero-Cuevas et al., 2009). It is known that biomechanically, the control of individual joints is
55 limited by the redundant set of muscles that control single or several joints (Lang and Schieber, 2004;
56 Rácz et al., 2012). Studies of neural and neuromuscular architecture of the hand have demonstrated
57 that these do not support fully isolated joint movements (Lemon, 1997; Poliakov and Schieber, 1999;
58 Reilly and Schieber, 2003), and biomechanical constraints appear to result in all muscles being
59 required for full directional control of grip forces (Kutch and Valero-Cuevas, 2011). Additionally, it
60 has been proposed that motor control of the hand joints is organized in a modular way, where several
61 degrees of freedom are organized into functional groups to simplify the control problem (Santello et
62 al., 1998; Tresch et al., 2006).

63 In the realm of muscle co-actions so called motor synergies were identified to represent structured
64 spatio-temporal patterns of muscle interplay in defined movements (Bernstein, 1967; Santello et al.,
65 2002; Daffershofer et al., 2004; d'Avella et al., 2006; Tresch et al., 2006). Also, studies that have
66 focused on finger joint kinematics of complex hand shapes (Santello et al., 1998; Mason et al., 2001;
67 Daffertshofer et al., 2004), as well as continuous daily-life-day activity (Ingram et al., 2008) found
68 that most variability in the data could be explained by just a few (four to six) characteristic
69 parameters (so called principal components) that indicates a high degree of correlation between the
70 angles of the fingers. These have also been replicated in studies focusing on the key evolutionary
71 ability to produce flint-stone tools (Faisal et al., 2010).

72 The importance of the hand as our means to interact with the world becomes painfully evident
73 when loss of a hand or hand function occurs. Here neuroprosthetics and robotic hands have rapidly
74 evolved to imitate an unprecedented level of hand-control (Wolpaw and McFarland, 1994; Taylor et
75 al., 2002; Wolpaw and McFarland, 2004; Hochberg et al., 2006; Bitzer and van der Smagt, 2006;
76 Carrozza et al., 2006; Zhou et al., 2007; Kuiken et al., 2007; Steffen et al., 2007; Rothling et al.,
77 2007; Cipriani et al., 2008; Velliste et al., 2008; Lui et al., 2008; Schack and Ritter, 2009; Kuiken et
78 al., 2009; Hochberg et al., 2012; Schröder et al., 2012; Feix et al., 2013; Thomik et al., 2013). Yet, it
79 is still very difficult for people with a lost limb to achieve naturalistic mobility and dexterity by
80 controlling a prosthetic replacement in the same way they would control their own body. This
81 increases the training time to use such neuroprosthetics (up to two years) and results in a low
82 adoption rate after training.

83 We hypothesize that natural hand movements performed “in-the-wild”, outside artificially
84 construed and highly controlled laboratory tasks contain correlation information that can be used for
85 prediction and reconstruction in the context of prosthetics. We asked subjects to perform everyday
86 tasks such as opening the door, eating, using the phone, etc. The data consists of 15-dimensional time
87 series representing the angles of all the major joints of all the fingers. Advances in experimental
88 methods have increased the availability, amount and quality of high-resolution behavioural data for

89 both humans and animals that can be collected. However, most behavioural studies lack adequate
90 quantitative methods to model behaviour and its variability in a natural manner. Here, we take the
91 view that motor behaviour can be understood by identifying simplicity in the structure of the data,
92 which may reflect upon the underlying control mechanisms. Yet, the analysis of movements and
93 specifically hand movements is complicated by the highly variable nature of behaviour (Faisal et al.,
94 2008). To extract the structure of hand configuration variability data stream we used a probabilistic
95 generative latent variable model (PPCA) of hand configurations for each task.

96 Part of these results was previously published in the form of abstracts (Belić and Faisal, 2011;
97 Belić and Faisal, 2014).

98

99 **2. Materials and methods**

100 **2.1. Subjects**

101 Seven adults (two women and five men, average age 24 ± 2 years) with no known history of
102 neurological or musculoskeletal problems, participated in this study following approved ethical
103 guidelines. All subjects were right-handed as determined by the Edinburgh Handedness Inventory
104 (Oldfield, 1971). The experimental procedure used in this experiment was approved by the local
105 ethics committee.

106

107 **2.2. Experiments and data acquisition**

108 We asked subjects to perform 17 different everyday tasks (Figure 1), while capturing their hand
109 movements by using resistive sensors embedded in a previously calibrated CyberGlove I
110 (CyberGlove System LLC, CA, USA). The data glove is made of thin cloth, and its sensors are
111 correlated with corresponding joints of the human hand (Figure 2A). The CyberGlove we used in this
112 study is associated with 18 DOF of the hand. We used data from 15 sensors that consisted
113 of metacarpalphalangeal (MCP) and proximal interphalangeal (PIP) sensors for the four fingers, three
114 stretch sensors between the four fingers, three sensors for the thumb (the carpometacarpal (CMC),
115 MCP and interphalangeal (IP) sensors), and the stretch sensor between the thumb and the palm of the
116 hand. Sensors were sampled continuously at 80 Hz at a resolution of 8 bits per sensor. Subjects
117 completed 10 repetitions for each of the activities, and they always started trials from the same initial
118 position (the hand was placed on the interface device attached to the subject's belt with the fingers
119 composed together and thumb oriented parallel to the palm). The beginning of each trial was
120 indicated with a sound. The trials were self-paced and the purpose of activities was explained to
121 subjects orally, but they were not instructed about any desired movements for the upcoming trials.
122 After performing the task, the subject then returned his/her hand to the initial position. All programs
123 for data acquisition, visualization and calibration were purpose-developed in C++.

124

125 **2.3. Calibration**

126 The output of each CyberGlove sensor is voltage value (raw value) which is dependent on the
127 bending applied to that specific sensor. In order to obtain the outputs in degrees (Figure 2B), it is
128 necessary to determine conversion factor gain and a constant term offset for each of the sensors. This

129 process is called calibration of the CyberGlove. Once the gain and offset are set, output in degrees of
130 the corresponding sensor is given by the following equation:

$$angle = gain * (RawValue - offset).$$

131 To calculate the gain and offset we need two different pre-defined angles for each of the sensors
132 and raw values that correspond to them ($RawValue_1$ and $RawValue_2$). Gain and offset are calculated
133 by the following formulas:

$$gain = \frac{(angle_1 - angle_2)}{(RawValue_1 - RawValue_2)},$$

$$offset = RawValue_1 - \frac{angle_1}{gain}.$$

134 The glove was calibrated for each subject using a five-step procedure that allowed us to determine
135 two different angles ($angle_1$ and $angle_2$) for each of the sensors (Figure 3):

136 The first position corresponded to 0° for all glove sensors (Figure 3A).

137 The second position defined an angle of 90° for all MCP sensors except for the thumb (Figure 3B).

138 The third position determined the abduction angles of 30° between the middle and index finger and
139 between the little and ring finger, an angle of 20° between the ring and middle finger, and an angle of
140 90° between the index and thumb finger.

141 The fourth position defined an angle of 90° for all PIP sensors except for the thumb.

142 The fifth position corresponded to the angles for the thumb sensors: CMC (90°), MCP (45°) and IP
143 (90°) sensor.

144 The calibration procedure was further improved using an online visualization system. In our study,
145 a virtual human hand was rendered in OpenGL. The virtual hand was animated in real-time by data
146 from the glove (Figure 3F). Visualization of data was of great help during both calibration and data
147 acquisition processes. In the case of visually observed deviation between the 3D model and the actual
148 position of the hand, gain and offset were re-determined only for the sensors where deviation was
149 observed. Calibration parameters for each of the subjects had been stored in a separate file and loaded
150 before the experiments started. We also asked subjects, after completing the calibration procedure, to
151 again place their hand in the first position, so we could additionally check eventual discrepancies.
152 The average error across the sensors was 5 ± 2 degrees.

153

154 **2.4. Computational Latent Variable modelling of real-life movements**

155 Collected data from the 15 sensors for each subject and each trial were stored to disk for offline
156 analysis using MatLab (MathWorks, Natick (MA)). Before further analysis, the data is smoothed
157 using a second-order Savitzky-Golay filter with a running window of five data points to remove
158 discontinuities induced by the A/D converter.

159 Our data space potentially extends over a 15-dimensional space. We performed Principle
160 Component Analysis (PCA) on joint angles in order to estimate real dimensionality of the finger
161 movements during daily activities. PCA reduces the set of correlated variables to a set of non-
162 correlated variables (principle components) (Semmlow, 2001; Bishop 2006). The first principal
163 component contains as much of the variability (as quantified by the variance) in the data as possible,
164 as does each succeeding component for the remaining variability. Therefore, here we used the PCA
165 method to determine the complexity of the finger movements, by measuring how many principal

166 components can explain most of the variability in the data (Faisal et al., 2010). For example,
167 dimensionality reduction techniques can be illustrated by considering the index finger, which has
168 three joints controlled by five muscles. Describing the flexing behaviour of this finger requires *a*
169 *priori* three values (“dimensions”). For example, in specific movements like making a fist, as we flex
170 one joint of the index finger, we flex the other two joints at the same time in a highly coordinated
171 manner. Thus, we would require in principle a single dimension to describe the configuration of the
172 finger. PCA ignores the temporal structure of movements (in fact the results of PCA will be the same
173 if the data in each trial is randomly shuffled in time). Thus, correct classification relies on the sub-
174 space of finger movement variability alone.

175 Tipping and Bishop found a probabilistic formulation of PCA by viewing it as a latent variable
176 problem, in which a d -dimensional observed data vector \mathbf{x} can be described in terms of an m
177 dimensional latent vector, \mathbf{y} :

$$\mathbf{x} = \mathbf{W}\mathbf{y} + \boldsymbol{\mu} + \boldsymbol{\epsilon},$$

178 where \mathbf{W} is $d \times m$ matrix, $\boldsymbol{\mu}$ is the data mean and $\boldsymbol{\epsilon}$ is an independent Gaussian noise with a diagonal
179 covariance matrix \mathbf{I} . The likelihood of observed data vector \mathbf{x} is given as:

180

$$p(\mathbf{x}) = (2\pi)^{-d/2} |\mathbf{C}|^{-1/2} e^{(-1/2(\mathbf{x}-\boldsymbol{\mu})^T \mathbf{C}^{-1}(\mathbf{x}-\boldsymbol{\mu}))},$$

181 and \mathbf{Cov} is the model covariance matrix given by the following formula:

$$\mathbf{Cov} = \mathbf{W}\mathbf{W}^T + \sigma^2 \mathbf{I}.$$

182 \mathbf{W} and σ are obtained by iterative maximization of log-likelihood of p :

$$\sigma^2 = \frac{1}{d-m} \sum_{k=m+1}^d \gamma_k,$$

$$\mathbf{W} = \mathbf{U}_m (\mathbf{A}_m - \sigma^2 \mathbf{I})^{\frac{1}{2}} \mathbf{R},$$

183 where γ_k are eigenvalues, \mathbf{U}_m is $d \times m$ matrix of eigenvectors, \mathbf{A}_m is diagonal matrix ($m \times m$) of
184 eigenvalues, and \mathbf{R} is an arbitrary $m \times m$ orthogonal rotation matrix (for simplicity \mathbf{R} is usually equal
185 to \mathbf{I}).

186

187 2.5 Measure of manipulative complexity

188 As a way to quantify manipulative complexity for a given number of PCs, we proposed a universally
189 applicable measure that allowed us to calculate and compare limb movements across different tasks.
190 We refer to it as manipulative complexity C , and define the measure by the following formula:

$$C = 1 - \frac{2}{N-1} \sum_{j=1}^N \sum_{i=1}^j (\text{Variance explained by } PC_i - 1/N),$$

191 where N is the total number of PCs we consider. Our data space extends over a 15-dimensional
192 space, so if all PCs contribute equally that implies $C=1$, and $C=0$ if one PC explains all data
193 variability. Our complexity measure compares well with intuitive complexity estimates and it can be

194 thought of as a new assessment measure that is calculated after an objective mathematical analysis.
195 For example, a simple behaviour, e.g. curling and uncurling a hand into a fist, would reveal a single
196 dominant principal component as all 5 fingers (and each finger's joint) move in a highly correlated
197 manner and therefore C would be close to 0. In contrast, a complex behaviour, such as expert typing
198 on a keyboard would reflect more uniform distribution of variances explained by principal
199 components, as each finger moves independently from the others, and so C would have a high value.

200

201 **2.6 Task recognition from movement data (Bayesian classification)**

202

203 Next, we simply predicted a task based on the one with the highest PPCA likelihood by employing
204 Bayesian classifier. In Bayesian statistics there are two important quantities: unobserved parameters
205 Ω_j ($j=1, \dots, 17$ different activities in our study) and observed data \mathbf{x} (movement data). They are related
206 in the following way:

$$P(\Omega_j|\mathbf{x}) = \frac{P(\mathbf{x}|\Omega_j)P(\Omega_j)}{P(\mathbf{x})},$$

207

208 where $P(\Omega_j|\mathbf{x})$, which is termed posterior, represents probability that testing data \mathbf{x} belong to activity
209 Ω_j . Prior, $P(\Omega_j)$, is simply given by the relative frequency of occurrence of each class in the training
210 set and we can ignore it here. Therefore probability of each class, given testing data, is equal to
211 likelihood $P(\mathbf{x}|\Omega_j)$ (probability of seeing the data given the task) that is thoroughly explained in
212 section 2.4.

213 For training and testing the classifier we used leave-one-repetition (across all actions and all
214 subjects)-out cross-validation.

215

216 **2.7 Missing limb movement reconstruction (Latent variable decoding)**

217

218 For data reconstruction, firstly we used linear regression to fit the data of missing joints as a
219 function of other joints and expressed results as the average difference between actual and predicted
220 values. Then, we employed the Expectation-Maximization (EM) algorithm for PPCA in order to
221 estimate missing values and at the same time to determine the right subspace dimension. In the EM
222 approach for PPCA, we considered the latent variables \mathbf{y}_n to be 'missing' data and the 'complete'
223 data to encompass the observations together with these latent variables (Tipping and Bishop, 1999).
224 The corresponding complete-data log-likelihood is given as:

$$L_C = \sum_{n=1}^N \ln(p(\mathbf{x}_n, \mathbf{y}_n)),$$

$$p(\mathbf{x}_n, \mathbf{y}_n) = (2\pi\epsilon^2)^{-d/2} e^{-\frac{\|\mathbf{x}_n - \mathbf{W}\mathbf{y}_n - \boldsymbol{\mu}\|^2}{2\epsilon^2}} (2\pi)^{-m/2} e^{-\frac{\|\mathbf{y}_n\|^2}{2}}.$$

225 Then we calculated the expectation (E-step) of L_C :

$$\langle L_C \rangle = - \sum_{n=1}^N \left\{ \frac{d}{2} \ln(\sigma^2) + \frac{1}{2} \text{tr}(\langle \mathbf{y}_n \mathbf{y}_n^t \rangle) + \frac{1}{2\sigma^2} (\mathbf{x}_n - \mu)^t (\mathbf{x}_n - \mu) - \frac{1}{\sigma^2} \langle \mathbf{y}_n \rangle^t \mathbf{W}^t (\mathbf{x}_n - \mu) + \frac{1}{2\sigma^2} \text{tr}(\mathbf{W}^t \mathbf{W} \langle \mathbf{y}_n \mathbf{y}_n^t \rangle) \right\}, \text{ where}$$

$$\langle \mathbf{y}_n \rangle = \mathbf{C}^{-1} \mathbf{W}^t (\mathbf{x}_n - \mu),$$

$$\langle \mathbf{y}_n \mathbf{y}_n^t \rangle = \sigma^2 \mathbf{C}^{-1} + \langle \mathbf{y}_n \rangle \langle \mathbf{y}_n \rangle^t.$$

226 In the M-step, L_C was maximized with respect to \mathbf{W} and σ^2 :

$$\bar{\mathbf{W}} = \left[\sum_n (\mathbf{x}_n - \mu) \langle \mathbf{y}_n \rangle^t \right] \left[\sum_n \langle \mathbf{y}_n \mathbf{y}_n^t \rangle \right]^{-1}$$

$$\bar{\sigma}^2 = \frac{1}{Nd} \sum_{n=1}^N \left\{ \|\mathbf{x}_n - \mu\|^2 - 2 \langle \mathbf{y}_n \rangle^t \bar{\mathbf{W}}^t (\mathbf{x}_n - \mu) + \text{tr}(\langle \mathbf{y}_n \mathbf{y}_n^t \rangle \bar{\mathbf{W}}^t \bar{\mathbf{W}}) \right\}$$

227 These equations were iterated until the algorithm was judged to have converged.

228

229 3. Results

230 3.1 Natural hand and finger joint kinematics have a low-dimensional embedding

231

232 The structure of natural hand and finger movements in daily-life is characterized by a highly variable
 233 nature. Even in the case of handshaking (Figure 1G), which represents one of the most stereotypic
 234 actions, basic statistical analysis has revealed vast diversity in angular data for MCP and PIP joints
 235 across different subjects (Figure 4A). In this work we first exploited the correlations between MCP
 236 and PIP joints for each of the four fingers and we found that correlation coefficients were stronger for
 237 little and ring fingers and weaker for middle and index fingers (Figure 4B). Further, correlations
 238 between each of the four fingers were highest for the neighbouring fingers and gradually decreased
 239 for more distant fingers (Figure 4C). We also used Principal Component Analysis in order to estimate
 240 dimensionality of the finger movements across different complex manipulation tasks. Therefore, we
 241 used PCA as a measure for the complexity of hand configuration, by measuring the amount of
 242 variance in the data displayed by each of the principal components. For example, a simple behaviour
 243 such as curling and uncurling the hand would reveal a single dominant PC component, as all finger
 244 joints move in a highly correlated manner. In Figure 5A we show the percentage of explained
 245 variance versus the number of used principal components for each of the 17 activities. PCA revealed
 246 for all tasks that hand motor control restricted hand configurations on a low dimensional subspace of
 247 four to five dimensions (which explained 83-96% of the variance in the data), in line with previous
 248 data on evolutionary relevant hand behaviour (crafting of flint stone tools, Faisal et al., 2010) and
 249 non-annotated long-term statistics of joint velocities (Ingram et al., 2008). These results imply a
 250 substantial reduction from the 15 degrees of freedom that were recorded. Some of the activities

251 required more principal components than others to reconstruct the data. For example in Figure 5A we
252 can see that opening a lid on a bottle or manipulating a fork are far more complex activities than hand
253 dialling numbers on a phone. Single PC component explained around 30% less variance in the first
254 case (opening a lid) than in the second (dialling numbers), while that discrepancy was around 10% in
255 the case when we used only the first four PCs to explain variance.

256

257 **3.2 Measuring the manipulative complexity of activities in daily life**

258

259 We can visually observe some differences and similarities in the manipulative complexity between
260 the most simple hand movements, during which the individual joints move in a highly correlated
261 manner, and the most complex, where each finger moves independently from the others. Here we
262 proposed a universally applicable measure of manipulative complexity (C) that allows us to measure
263 this quantity across vastly different tasks. Our complexity measure implies that $C=1$ if all DOF
264 contribute equally (the most complex activities), and $C=0$ if one DOF explains all DOF (the most
265 simple activities). Results produced are in line with intuitive expectations (opening a lid on a bottle is
266 more complex than operating a door handle) (Figure 5B). Some of the activities in our study also
267 included “grasp like motions” (e.g. operating a door handle, grabbing a bottle or grabbing a bag) that
268 visually would look very similar. Our established complexity measure appeared sensitive enough and
269 was able to differentiate between even those similar looking grasps.

270

271 **3.3 Prediction of hand movements from initial movement data**

272

273 Further, we wanted to see how different subspaces influence success of classification for different
274 tasks. To deal with this, we used Bayesian PPCA. PPCA has been considered as a mechanism for
275 probabilistic dimension reduction or as a variable-complexity predictive density model (Tipping and
276 Bishop, 1999) and correct classification relies on the subspace of finger movement variability alone.
277 Figure 6A illustrates the success of classification with reference to the number of PPCA components.
278 Therefore, by using only the first few PPCA components in the classification process we can get very
279 high classification success. For example, using the first four PPCA components the success of
280 classification was 89.91% (across all tasks, classification performance was 96.63% using all 15
281 PPCA components). Importantly, in Figure 5 one could see that extracted subspaces appeared to be
282 task-dependant, which suggests that besides simplification, synergies might have a role in a task-
283 optimal control as well. If specific tasks can engage specific motor control strategies, then we should
284 be able to make a conclusion regarding the task by observing some early portions of finger data.
285 Indeed, the classification performance, presented in Figure 6B, was a few times higher than the
286 chance performance (marked with red line) for only an initial portion of the finger configuration
287 samples of each task. Within the first 1000ms from the initial hand position, which was identical for
288 every action, it appeared that hand shape already configures itself to a specific task and we were able
289 to quickly predict intended action. Vertical lines represent average duration for each of 17 activities.

290

291 **3.4 Reconstruction of missing limbs' movements by decoding movements of remaining limbs**

292

293 Next, we investigated the predictability of a subset of joint movements in respect of the movements
294 of other joints. Or in other words, if part of a limb is missing, how well can we predict what those
295 missing parts should be doing by only observing the intact, remaining limb parts. This is of
296 fundamental interest in prosthetic control. We focused particularly on cases where data had been
297 acquired with sensors that measure the bending around the MCP or the PIP joints of the four missing
298 fingers. First, we applied linear regression in the case of missing values from the MCP joints (Figure
299 7A) and the PIP joints (Figure 7B) for each of the four fingers separately. The error we got, measured
300 as absolute difference between predicted and actual joint values and averaged across all tasks,
301 showed the best linear predictability for the middle and ring fingers in both examined cases. Overall
302 predictability rate was high regarding movement range (90 °) for each of the considered joints and
303 variability of tasks. Then, we applied an EM algorithm for PPCA to infer the un-observed, invisible
304 joints in the case of missing data from the MCP sensors. Figure 7C shows obtained results with
305 reference to the number of PPCA components. Here the best results were also acquired for the middle
306 and ring fingers. The error was the highest in the case when just one PPCA component was used and
307 then started to decrease (up to a number around 8 PPCA). Generally, these results could help us to
308 improve the method of designing prosthetic controllers that are driven by intact limb parts and
309 support neuroprosthetic controllers in refining the decoding of action intention of users.

310

311 **4. Discussion**

312

313 We analysed natural movements from the seven subjects who were behaving spontaneously while
314 performing 17 different everyday activities. We have four key findings that we will discuss
315 individually in more detail as follows: 1. Regarding activities of daily living, we confirmed that hand
316 control is low-dimensional, i.e. four to five PCs explained 80-90% of the variability in the movement
317 data. 2. We established a universally applicable measure of manipulative complexity that allowed us
318 to measure this quantity across vastly different tasks. Our findings are in line with intuitive
319 expectations (opening a lid on a bottle is more complex than hand dialling numbers) and are sensitive
320 enough to differentiate between similar looking interactions (e.g. operating a door handle is less
321 complex than grabbing a bottle). 3. We discovered that within the first 1000ms of an action the hand
322 shape already configures itself to vastly different tasks, enabling us to reliably predict the action
323 intention. 4. We suggest how the statistics of natural finger movements paired with Bayesian latent
324 variable model can be used to infer the movements of missing limbs from the movements of the
325 existing limbs to control for example, a prosthetic device.

326 In many everyday activities we move our fingers in a highly correlated manner. Therefore, it has
327 been proposed that control of human hand movements is organized in a way that comprises coupling
328 of several DOF into functional groups. The opinion that motor synergies lie behind manual actions
329 has been supported by several studies (Santello et al., 1998; Santello et al., 2002; Daffershofer et al.,

330 2004; d'Avella et al., 2006; Tresch et al., 2006; Ingram et al., 2008; Faisal et al., 2010; Jarrasse et al.,
331 2014). The most common interpretation is in terms of simplifying the strategy that the central
332 nervous system might undertake. Studies that have investigated hand configurations during reaching
333 and grasping movements (Santelo et al., 1998; Mason et al., 2001) reported that 90% of the variance
334 in hand configurations could be explained by only three principal components. In our study PCA
335 analysis revealed that in 17 daily activities hand configurations operated on low-dimensional
336 subspace (four to five dimensions) as well, which is also in line with previous data on evolutionary
337 relevant hand behaviour (crafting of flintstone tools) (Faisal et al., 2010) and non-annotated long-
338 term statistics of joint velocities (Ingram et al., 2008). These finding supports the view that the motor
339 cortex organizes behaviour in a low-dimensional manner to avoid the curse of dimensionality in
340 terms of computational complexity. We also found numerical differences in the number of principle
341 components required to explain a given amount of variability in hand configurations across each of
342 the tasks. Similar conclusions were obtained in the case of a small number of much simpler
343 manipulation tasks (Todorov and Ghahramani, 2004; Bläsing et al., 2013).

344 Our manipulative complexity measure, established for the first time, gave us a chance to quantify
345 the complexity of the movements across a high number of different activities. This was very
346 important in that some of the activities that look highly similar (grasp like motions such as operating
347 a door handle, grabbing a bottle or grabbing a bag) apparently had different values of complexity.
348 Those findings demonstrated also that our complexity measure is sensitive enough to differentiate
349 between similar looking interactions. The highest value of complexity had tasks of opening a lid on a
350 bottle or manipulating a fork, and the lowest had tasks of dialling numbers on a phone or opening a
351 door using the door knob. Results produced are in line with intuitive expectations regarding the fact
352 that in the first two cases one is expected to have high engagement of the thumb that is the most
353 individuated (Häger-Ross and Schieber, 2000). In the case of typing numbers, most of the subjects
354 used their index finger while their other fingers created some form of fist, and in case of opening the
355 door our fingers move in a highly correlated manner. Here we compare structures of complex
356 dynamic hand manipulations, while some other studies (Feix et al., 2009; Feix et al., 2013) have
357 presented a successful methodology for measuring and evaluating the capability of artificial hands to
358 produce 31 different human-like grasp postures.

359 Further we employed Bayesian PPCA on the behavioural data in order to analyse the structure of
360 variability within it. Variability is ubiquitous in the nervous system and it has been observed in
361 actions even when external conditions are kept constant (Faisal et al., 2008). In this paper we take the
362 view that the hand configuration variability may contain significant information about the task being
363 performed. Our approach yields an effective assessment of the tasks that subjects were involved with.
364 The Bayesian PPCA reveals that the finger movement correlations are so structured that we can
365 obtain very high classification success by taking only first few principal components. Regarding
366 motor control, it has been suggested that structural learning (Braun et al., 2009) may reduce the
367 dimensionality of the control problem that the learning organism has to search in order to adapt to a
368 new task. Our results are in line with this concept and suggest the hypothesis that the brain can
369 engage many sets of motor controllers, which are selected based on specific tasks, and which also
370 orchestrate resulting actions in overall behaviour and produce movement variability in characteristic
371 sub-spaces. Next we thought that, if the hypothesis is true, we should be able to infer the task the

372 hand is engaged in by observing some initial portion of the finger movement data. Crucially,
373 observing only the initial portion of hand configurations (from our identical starting position) was
374 sufficient to characterize the entire hand task, and the classification performance we obtained was a
375 few times higher than chance performance.

376 A common approach in design of Neuroprosthetics is to construct body parts that can be
377 controlled with the same functionality as natural limbs. Using a reduced set of basic functions to
378 construct internal neural representation could be essential from an optimal control perspective
379 (Poggio and Bizzi, 2004) and applied to Neuroprosthetics control (Thomik, et al., 2013). Our linear
380 predictability of the missing joints based on movements of other finger joints gave good results. The
381 best results were achieved for middle and ring fingers showing that they are the least individuated.
382 This is in line with the previous research (Häger-Ross and Schieber, 2000). Further, the PPCA
383 algorithm for missing data revealed that using more than eight PPCA components does not lead to
384 any significant improvement. In this study we perform action recognition and reconstruction of
385 missing finger trajectories using the current positions of other functional finger joints by simply
386 requiring – in principle – the user to act out with his functional fingers an intended task. Such finger
387 motion can be realized with cheap wearable wireless sensors (Gavriel and Faisal, 2013) and we can
388 reconstruct the natural behaviour of users without the need for expensive, training intensive, non-
389 invasive or invasive electrophysiological interfaces. Consequently, unlike common approaches that
390 require the user to learn to use the technology, the technology interprets the natural behaviour of
391 users (Abbott and Faisal, 2011). Thus, the neuronal and biomechanically imposed correlation
392 structure of hand-finger can be exploited to build smart, sensitive Neuroprosthetics controllers that
393 infer the task “at hand” based on the movements of the remaining joints.

394 Dexterous object manipulation is conditioned by the continuous interactions between the body and
395 the environment and engages multiple sensory systems. Vision can provide essential information for
396 controlling hand kinematics in the cases when object are fully visible. Human manipulation involves
397 also tactile signals from different types of mechanoreceptors in the hand that allows humans to easily
398 hold a very wide range of objects with different properties without crushing or dropping them
399 (Johansson and Flanagan, 2009). Tactile sensing provides also critical information in avoiding
400 slipping as crucial precondition to successfully manipulate an object, what is most apparent in people
401 with impaired tactile signals. When finger contact with the desired object is made, we start to
402 increase the grasp force to the optimal level, using both our prior knowledge about the object and
403 information from the tactile sensors of the fingers gathered during the interaction (Johansson and
404 Flanagan, 2008; Romano et al., 2011). Corrective actions are applied to different frictional conditions
405 in order to provide an optimal grip force that is normally 10–40% greater than the minimum required
406 to prevent slips (Johansson and Flanagan, 2008). Consequently, future Neuroprosthetics should
407 provide reliable user’s intention decoding as well as optimal sensory feedback (Berg et al., 2013;
408 Raspovic et al., 2014). Therefore, looking into hand kinematics as an important aspect of the hand
409 capabilities represents just one approach that forms the basis for future studies. Further inclusion of
410 other parameters that are of relevance and investigating their influence on manipulative complexity
411 will provide a more complete analysis.

412

413

414 **5. Acknowledgments**

415 JJB was supported by the IASTE scholarship of the British Council. AAF acknowledges the
416 support of the Human Frontiers Program Grant (HFSP RPG00022/2012).

417

418 **6. References**

- 419 Napier, J. (1980). *Hands*. New York: Pantheon Books.
- 420 Tubiana, R. (1981). " Architecture and function of the hand". In: *The Hands*, ed. R. Tubiana
421 (Philadelphia, PA: Saunders), 19-93.
- 422 Stockwell, R.A. (1981). "Joints". In: *Cunningham's text-book of anatomy*, ed. G.J. Romnes, (Oxford:
423 Oxford University Press), 211-264.
- 424 Soechting, J.F., Flanders, M. (1997). Flexibility and repeatability of finger movements during
425 typing: analysis of multiple degrees of freedom. *J Comput Neurosci* 4, 29-46.
- 426 Jones, L.A., Lederman, S.J. (2006). *Human Hand function*. Oxford: Oxford University Press.
- 427 Todorov, E., Ghahramani, Z. (2004). Analysis of the synergies underlying complex hand
428 manipulation. *IEEE Conf Proc EMBS* 6, 4637-4640.
- 429 Weiss, E., Flanders, M. (2004). Muscular and Postural Synergies of the Human Hand.
430 *J. Neurophysiol.* 92, 523-535.
- 431 Ingram, J., Kording, K., Howard, I., Wolpert, D. (2008). The statistics of natural hand movements.
432 *Exp. Brain Res.* 188, 223-236.
- 433 Valero-Cuevas, F., Venkadesan, M., Todorov, E. (2009). Structured Variability of Muscle
434 Activations Supports the Minimal Intervention Principle of Motor Control. *J. Neurophysiol.*
435 102, 59-68.
- 436 Lang, C.E., Schieber, M.H. (2004). Human finger independence: limitations due to passive
437 mechanical coupling versus active neuromuscular control. *J. Neurophysiol.* 92, 2802–2810.
- 438 Rácz, K., Brown, D., Valero-Cuevas, F. (2012). An involuntary stereotypical grasp tendency pervades
439 voluntary dynamic multifinger manipulation. *J. Neurophysiol.* 108, 2896-2911.
- 440 Lemon, R.N. (1997). Mechanisms of cortical control of hand function. *Neuroscientist* 3, 389–398.
- 441 Poliakov, A.V., Schieber, M.H. (1999). Limited functional grouping of neurons in the motor cortex
442 hand area during individuated finger movements: a cluster analysis. *J. Neurophysiol.* 82,
443 3488–3505.
- 444 Reilly K.T., Schieber, M.H. (2003). Incomplete functional subdivision of the human multi-tendon
445 finger muscle flexor digitorum profundus: an electromyographic study. *J. Neurophysiol.* 90,
446 2560–2570.
- 447 Kutch J.J., Valero-Cuevas, F.J. (2011). Muscle redundancy does not imply robustness to muscle
448 dysfunction. *J. Biomech.* 44, 1264-1270.
- 449 Santello, M., Flanders, M., Soechting, J.F. (1998). Postural hand synergies for tool use. *J Neurosci.*
450 18, 10105–10115.

- 451 Tresch, M.C., Cheung, V.C.K., d'Avella, A. (2006). Matrix factorization algorithms for the
452 identification of muscle synergies: evaluation on simulated and experimental data sets. *J*
453 *Neurophysiol.* 95, 2199–2212.
- 454 Bernstein, N. A. (1967). The co-ordination and regulation of movements. Oxford: Pergamon Press.
- 455 Santello, M., Flanders, M., Soechting, J.F. (2002). Patterns of hand motion during grasping and the
456 influence of sensory guidance. *J Neurosci.* 22, 1426–1435.
- 457 Daffertshofer, A., Lamoth, C.J., Meijer, O.G., Beek, P.J. (2004). PCA in studying coordination and
458 ariability: a tutorial. *Clin. Biomech.* 19, 415–428.
- 459 d'Avella, A., Portone, A., Fernandez, L., Lacquaniti, F. (2006). Control of fast-reaching movements
460 by muscle synergy combinations. *J Neurosci.* 26, 7791–7810.
- 461 Mason, C.R., Gomez, J.E., Ebner, T.J. (2001). Hand synergies during reach-to-grasp. *J Neurophysiol.*
462 86, 2896–2910.
- 463 Faisal, A., Stout D., Apel, J., & Bradley, B. (2010). The Manipulative Complexity of Lower
464 Paleolithic Stone Toolmaking. *PLoS ONE* 5:6. doi: 10.1371/journal.pone.0013718.
- 465 Wolpaw, J. R., McFarland, D.J. (1994). Multichannel EEG-based brain-computer communication.
466 *Electroencephalogr. Clin. Neurophysiol.* 90, 444–449.
- 467 Taylor, D., Tillery, S.I.H., Schwartz, A.B. (2002). Direct cortical control of 3D Neuroprosthetic
468 devices. *Science* 296, 1829-1832.
- 469 Wolpaw, J.R., McFarland, D.J. (2004). Control of a two-dimensional movement signal by a
470 noninvasive brain-computer interface in humans. *Proceedings of the National Academy of*
471 *Sciences (USA)* 101, 17849–17854.
- 472 Hochberg, L.R., Serruya, M.D., Friehs, G.M., Mukand, J.A., Saleh, M., Caplan, A.H., Branner, A.,
473 Chen, D., Penn, R.D., Donoghue, J.P. (2006). Neural ensemble control of prosthetic devices
474 by a human with tetraplegia. *Nature* 442, 164-171.
- 475 Bitzer, S., van der Smagt, P. (2006). Learning EMG control of a robotic hand: Towards active
476 prostheses. *IEEE Conf Proc on Robotics and Automation (ICRA)*, 2819–2823.
- 477 Carrozza, M.C., Cappiello, G., Micera, S., Edin, B.B., Beccai, L., Cipriani, C. (2006). Design of a
478 cybernetic hand for perception and action. *Biol. Cybern.* 95, 629–644.
- 479 Zhou, P., Lowery, M.M., Englehart, K.B., Huang, H., Li, G., Hargrove, L., Dewald, J.P., Kuiken,
480 T.A. (2007). Decoding a new neural machine interface for control of artificial limbs. *J*
481 *Neurophysiol.* 98, 2974-2982.
- 482 Kuiken, T.A., Miller, L.A., Lipschutz, R.D., Lock, B.A., Stubblefield, K., Marasco, P.D., Zhou, P.,
483 Dumanian, G.A. (2007). Targeted reinnervation for enhanced prosthetic arm function in a
484 woman with a proximal amputation: a case study. *The Lancet* 369, 371–380.
- 485 Steffen, J., Haschke, R., Ritter H. (2007). Experience-based and tactile-driven dynamic grasp control.
486 In: *Intelligent Robots and Systems, 2007. IROS 2007. IEEE/RSJ International Conference on,*
487 2938-2943.
- 488 Rothling, F., Haschke, R., Steil, J. J., Ritter, H. (2007). Platform portable anthropomorphic grasping
489 with the bielefeld 20-DOF shadow and 9-DOF TUM hand. In: *Intelligent Robots and Systems,*
490 *2007. IROS 2007. IEEE/RSJ International Conference on,* 2951-2956.
- 491 Cipriani, C., Zaccone, F., Micera, S., Carrozza, M.C. (2008). On the shared control of an EMG-
492 controlled prosthetic hand: analysis of user-prosthesis interaction. *IEEE Trans Robotics* 24,

- 493 170–184.
- 494 Velliste, M., Perel, S., Spalding, M.C., Whitford, A.S., Schwartz, A.B. (2008). Cortical control of a
495 prosthetic arm for self-feeding. *Nature* 453, 1098-1101.
- 496 Liu, H., Wu K., Meusel, P., Seitz, N., Hirzinger, G., Jin, M.H., Liu, Y.W., Fan, S.W., Lan, T.,
497 Chen, Z.P. (2008). Multisensory five-finger dexterous hand: The DLR/HIT hand II. In: *Proc.*
498 *IEEE/RSJ Int. Conf. Intell. Robots Syst.*, 3692–3697.
- 499 Schack, T., Ritter, H. (2009). The cognitive nature of action — functional links between cognitive
500 psychology, movement science, and robotics. *Progress in Brain Research* 174, 231-250.
- 501 Kuiken, T.A., Li, G., Lock, B.A., Lipschutz, R.D., Miller, L.A., Stubblefield, K.A., Englehart, K.B.
502 (2009). Targeted muscle reinnervation for realtime myoelectric control of multifunction
503 artificial arms. *JAMA* 301, 619–628.
- 504 Hochberg, L.R., Bacher, D., Jarosiewicz, B. (2012). Reach and grasp by people with
505 tetraplegia using a neurally controlled robotic arm. *Nature* 485, 372-375.
- 506 Schröder, M., Elbrechter, C., Maycock, J., Haschke, R., Botsch, M., Ritter, J.H. (2012). Real-time
507 hand tracking with a color glove for the actuation of anthropomorphic robot hands. In: *IEEE-RAS*
508 *International Conference on Humanoid Robots (Humanoids)*, 262–269.
- 509 Feix, T., Romero, J., Ek, C. H., Schmiedmayer, H.B., Kragic, D. (2013). A Metric for Comparing
510 the Anthropomorphic Motion Capability of Artificial Hands. *IEEE Transactions on Robotics*
511 29, 82-93.
- 512 Thomik, A., Haber, D., Faisal, A. (2013). Real-time movement prediction for improved control of
513 neuroprosthetics. *IEEE/EMBS Conf Proc. Neural Engineering (NER)* 6, 625-628.
- 514 Faisal, A., Selen, L., Wolpert, D. (2008). Noise in the nervous system. *Nature Review Neuroscience*
515 9, 292-303.
- 516 Belić, J.J., Faisal, A.A. (2011). The structured variability of finger motor coordination in daily tasks.
517 *BMC Neuroscience*. doi:10.1186/1471-2202-12-S1-P102.
- 518 Belić, J.J., Faisal, A.A. (2014). Bayesian approach to handle missing limbs in Neuroprosthetics.
519 *Bernstein conference Göttingen*. doi: 10.12751/nncn.bc2014.0166.
- 520 Oldfield, R.C. (1971). The assessment and analysis of handedness: The Edinburgh inventory.
521 *Neuropsychologia* 9, 97-113.
- 522 Semmlow, J. (2001). *Biosignal and Biomedical Image Processing*. New York: Marcel Dekker, Ink.
- 523 Bishop, C. (2006). *Pattern Recognition and Machine Learning*. New York: Springer
524 Science+Business Media, LLC.
- 525 Tipping, M., Bishop, C. (1999). Probabilistic Principal Component Analysis. *Journal of the Royal*
526 *Statistical Society* 61, 611-622.
- 527 Harris, C. M., Wolpert, D. M. (1998). Signal-dependent noise determines motor planning. *Nature*
528 394, 780-784.
- 529 Jarrassé, N., Ribeiro, A.T., Sahbani, A., Bachta, W., Roby-Brami, A.(2014). Analysis of hand
530 synergies in healthy subjects during bimanual manipulation of various objects. *J. Neuroeng.*
531 *Rehabil.* 11, 1-11.
- 532 Bläsing, B., Maycock J., Bockemühl T., Ritter Helge, Schack T. (2013). Motor synergies and mental
533 representations of grasping movements. In: *ICRA 2013 Workshop on Hand synergies - how to*
534 *tame the complexity of grasping*.

- 535 Häger-Ross, C., Schieber, M.H. (2000). Quantifying the independence of human finger movements:
536 comparisons of digits, hands, and movement frequencies. *J. Neurosci.* 20, 8542-8550.
- 537 Feix, T., Pawlik, R., Schmiedmayer, H., Romero, J., Kragic, D. (2009). A comprehensive grasp
538 taxonomy. In: *Robotics, Science and Systems: Workshop on Understanding the Human Hand*
539 *for Advancing Robotic Manipulation*, 2-3.
- 540 Braun, D.A., Aertsen, A., Wolpert, D.M., Mehring, C. (2009). Motor task variation induces structural
541 learning. *Current Biology* 19, 352-357.
- 542 Braun, D.A., , Mehring, C., Wolpert, D.M. (2009). Structure learning in actions. *Behavioral Brain*
543 *Research* 206, 157-165.
- 544 Poggio, T., Bizzi, E. (2004). Generalization in vision and motor control. *Nature* 431, 768-774.
- 545 Gavriel, C., Faisal, A.A. (2013). Wireless kinematic body sensor network for low-cost
546 neurotechnology applications “in-the-wild”. *IEEE/EMBS Conf Proc. Neural Engineering*
547 *(NER)* 6, 1279-1282.
- 548 Abbott, W., Faisal, A. (2011). Ultra-low cost eyetracking as an high-information-throughput
549 alternative to BMIs. *BMC Neuroscience*. doi: 10.1186/1471-2202-12-S1-P103.
- 550 Johansson, R.S., Flanagan, J.R. (2009). Coding and use of tactile signals from the fingertips in object
551 manipulation tasks. *Nature Reviews Neuroscience* 10, 345–359.
- 552 Johansson, R. S., Flanagan, J. R. (2008). Tactile sensory control of object manipulation in humans.
553 In: *The Senses: a Comprehensive Reference* 6, ed. E. Gardner and J.H. Kaas (San Diego:
554 Academic), 67-86.
- 555 Romano, J.M., Hsiao, K., Niemeyer, G., Chitta, S., Kuchenbecher, K.J. (2011). Human-inspired
556 robotic grasp control with tactile sensing. *IEEE Transactions on Robotics* 27, 1-11.
- 557 Berg, J.A., Dammann, J.F., Tenore, F.V., Tabot, G.A., Boback, J.L., Manfredi, L.R., Peterson, M.L.,
558 Katyal, K.D., Johannes, M.S., Makhlin, A., Wilcox, R., Franklin, R.K., Vogelstein, R.J.,
559 Hatsopoulos, N.G., Bensmaia, S.J. (2013). Behavioral demonstration of a somatosensory
560 neuroprosthesis. *IEEE Trans. Neural Syst. Rehabil. Eng.*, 21, 500–507.
- 561 Raspopovic, S., Capogrosso, M., Petrini, F.M., Bonizzato, M., Rigosa, J., Pino, G.D., Carpaneto, J.,
562 Controzzi, M., Boretius, T., Fernandez, E., Granata, G., Oddo, C.M., Citi, L., Ciancio, A.L.,
563 Cipriani, C., Carrozza, M.C., Jensen, W., Guglielmelli, E., Stieglitz, T., Rossini, P.M.,
564 Micera, S. (2014). Restoring natural sensory feedback in real-time bidirectional hand
565 prostheses. *Sci. Trans. Med.*, 6, 22ra19.

566 7. Figure legends

567

568 **Figure 1 Subjects were involved in 17 different everyday activities.** (A) Opening and closing a
569 drawer. (B) Removing a bottle cap (unwinding and winding). (C) Turning the pages of a newspaper
570 (one page in each trial). (D) Picking up a plate, putting it on the marked location, and returning it to
571 the starting position. (E) Eating an apple (subject takes one bite of the apple) and returning the apple
572 to the starting position. (F) Manipulating a mouse in a pre-defined way. (G) Handshaking for a
573 duration of five seconds. (H) Dialling pre-defined numbers on telephone. (I) Typing pre-defined text
574 on a keyboard. (J) Manipulating a plug and returning it to the starting position. (K) Opening a door
575 using a key and returning the key to the starting position. (L) Picking up and putting down an object
576 using a fork. (M) Opening and closing a door using the knob. (N) Picking up a telephone handle. (O)
577 Picking up a plastic bottle, simulating drinking, and returning the bottle to the starting position. (P)

578 Picking up and putting down a bag. (Q) Picking up a glass with a handle, simulating drinking, and
579 returning the glass to the starting position.

580 **Figure 2 Data acquisition.** (A) CyberGlove sensor locations. (B) Calibrated output signals from the
581 CyberGlove for one of the activities.

582 **Figure 3 CyberGlove calibration procedures.** (A) The position defines $angle_1$ for all CyberGlove
583 sensors. (B) The position defines $angle_2$ for sensors that correspond to MCP joints of the four fingers.
584 (C) The position defines $angle_2$ for abduction sensors. (D) The position defines $angle_2$ for sensors that
585 correspond to PIP joints of the four fingers. (E) The position defines $angle_2$ for sensors that were used
586 to measure the position of the thumb. (F) Examples for real time capturing of finger movements by
587 using a 3D hand model that was developed to further improve accuracy of the calibration procedure.

588 **Figure 4 Basic statistics for one of the most stereotypic actions across all subjects and analysis**
589 **of correlations across all data.** (A) Mean and standard error of angular data for MCP and PIP joints
590 in the case of handshaking activity for a duration of five seconds. (B) Correlations between MCP
591 and PIP joints for each of the four fingers. (C) Correlations between each of the four fingers. *I* index
592 finger, *M* middle finger, *R* ring finger, *L* little finger, *MCP* metacarpalphalangeal joint, *PIP* proximal
593 interphalangeal joint.

594 **Figure 5 Principal component analysis (PCA) and quantitative measure of manipulative**
595 **complexity.** (A) Curves show the cumulative sum of variance (expressed in percentage) explained by
596 increasing the numbers of principal components separately for each of the 17 daily-life activities. The
597 x-axis corresponds to the number of PCs; the y-axis shows the percentage of the variance of the
598 finger movements explained by the respective number of PCs. (B) Our proposed quantitative
599 measure of manipulative complexity (manipulative complexity is maximal (equal to 1) if all DOF
600 contribute equally, and minimal (equal to 0) if one DOF explains all DOF).

601 **Figure 6 Data classification.** (A) Classification performance with reference to the number of PPCA
602 components. (B) Classification performance with reference to the number of data samples taken
603 (duration of activity). Performance by chance is marked with the red line and vertical lines represent
604 the average number of data samples (duration) for each of 17 activities.

605 **Figure 7 Data reconstruction.** (A) Average error after linear reconstruction in the case when data
606 from MCP sensors of the four fingers were missing. (B) Average error after linear reconstruction in
607 the case when data from PIP sensors of the four fingers were missing. (C) Results of data
608 reconstruction by using PPCA with reference to the different number of PC components used.

609

610

611

612



613

614

615

616

617

618

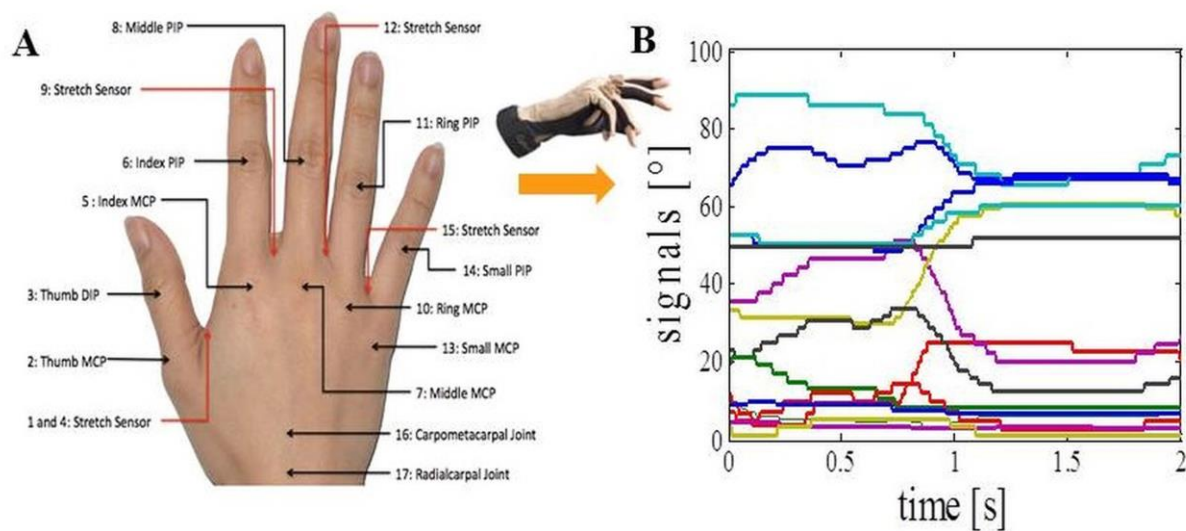
619

620

621

622

623



624

625

626

627

628

629

630

631

632

633

634

635

636

637

638

639

640

641



642

643

644

645

646

647

648

649

650

651

652

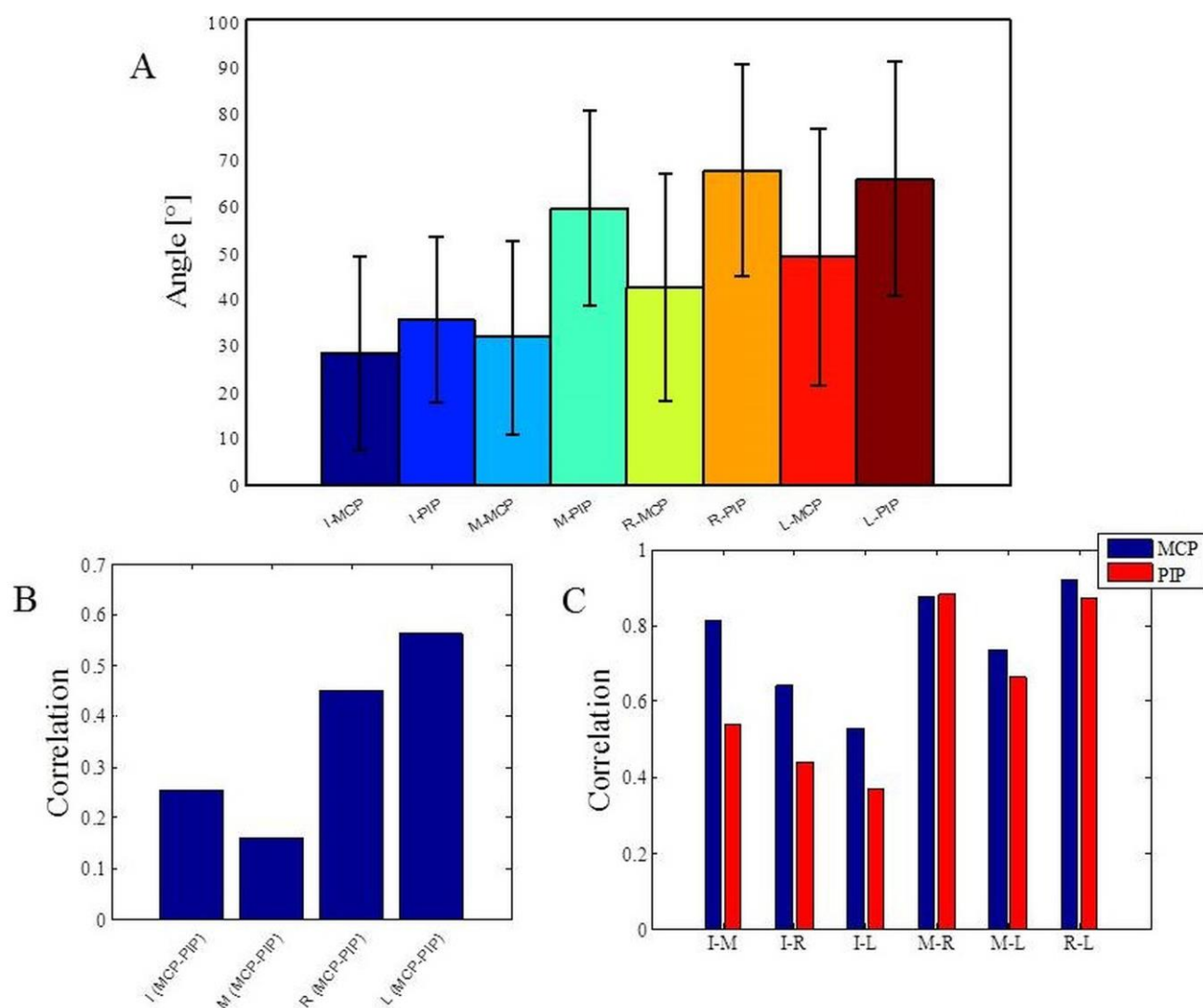
653

654

655

656

657



658

659

660

661

662

663

664

665

666

667

668

669

670

671

672

673

674

675

676

677

678

679

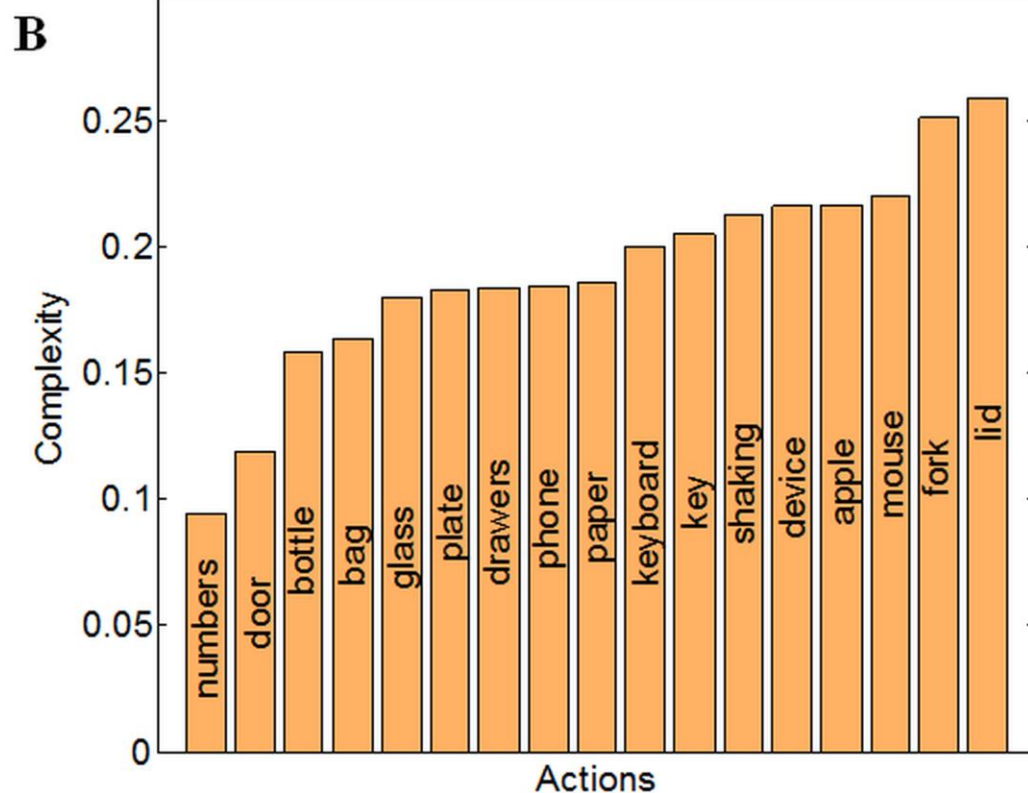
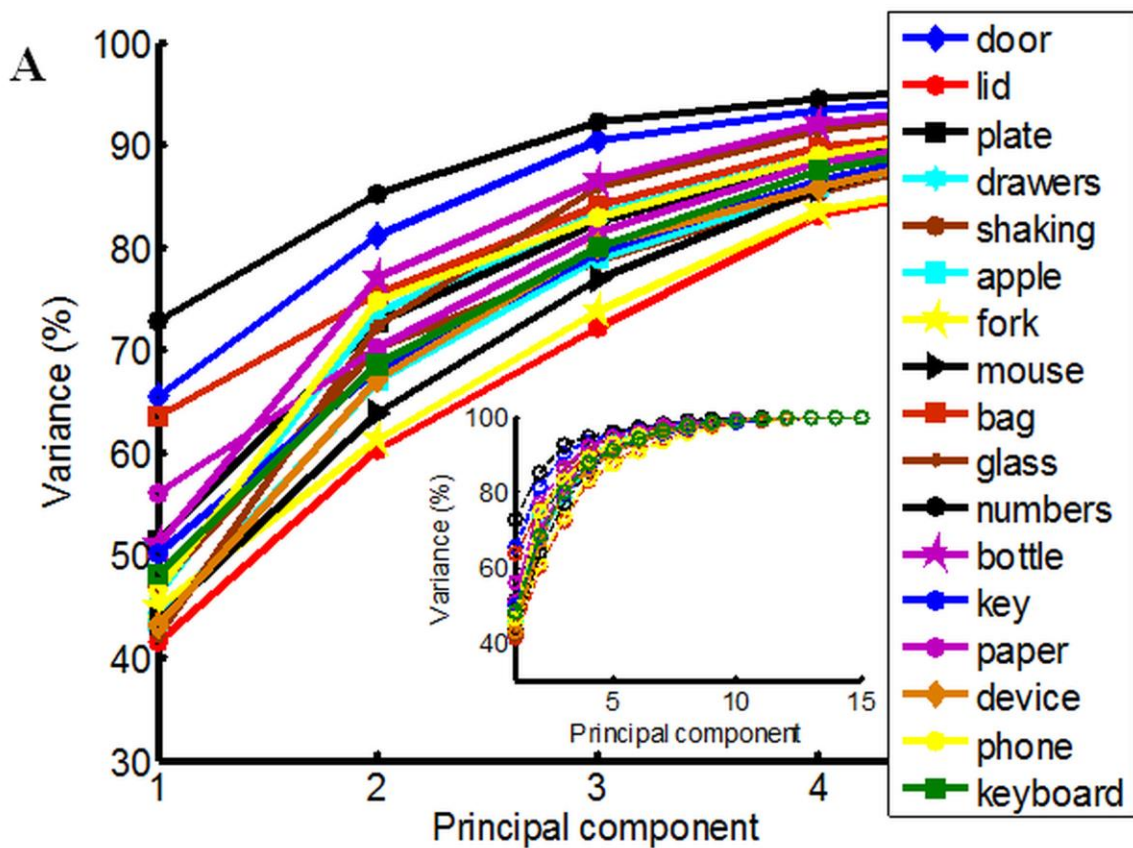
680

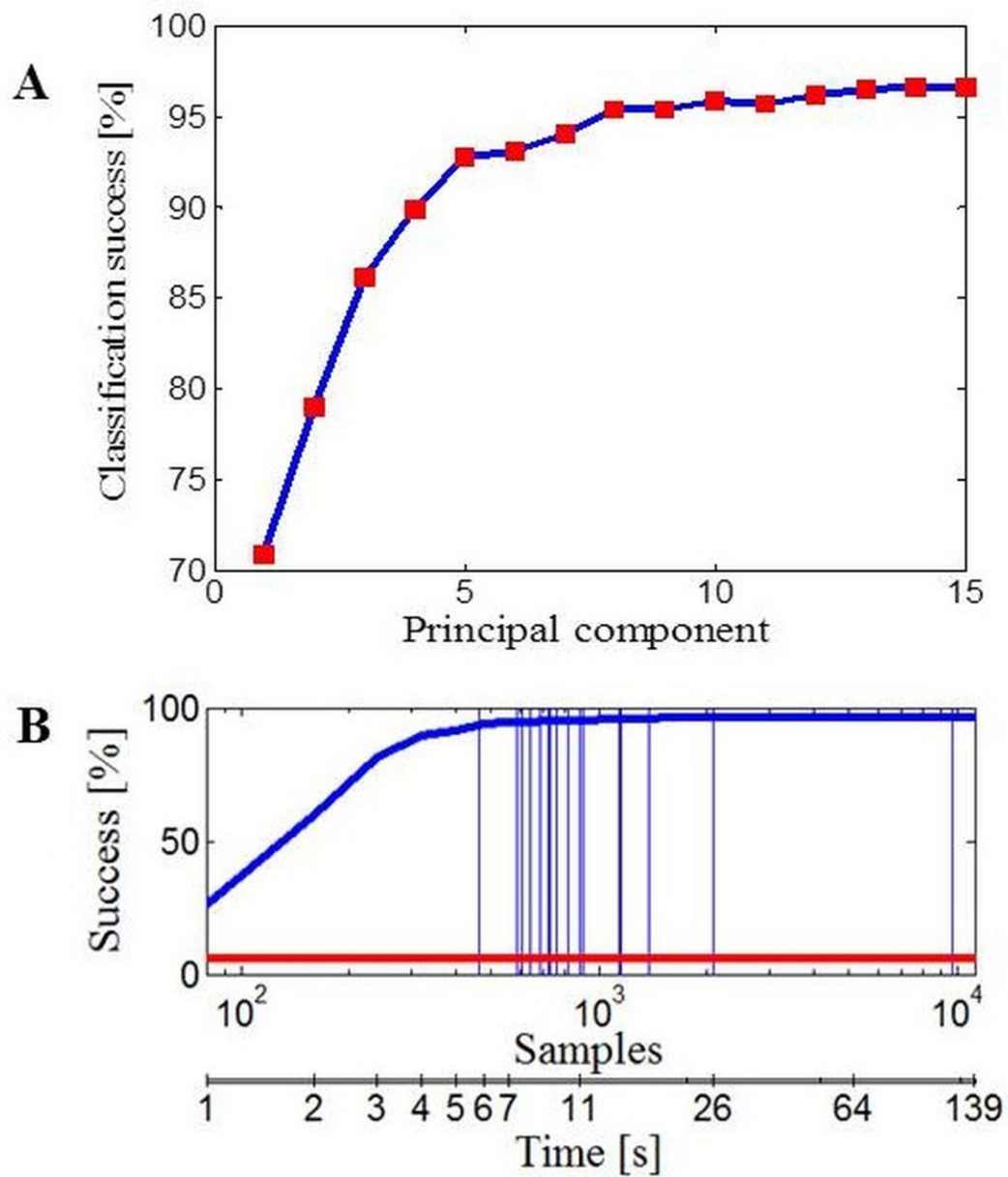
681

682

683

684





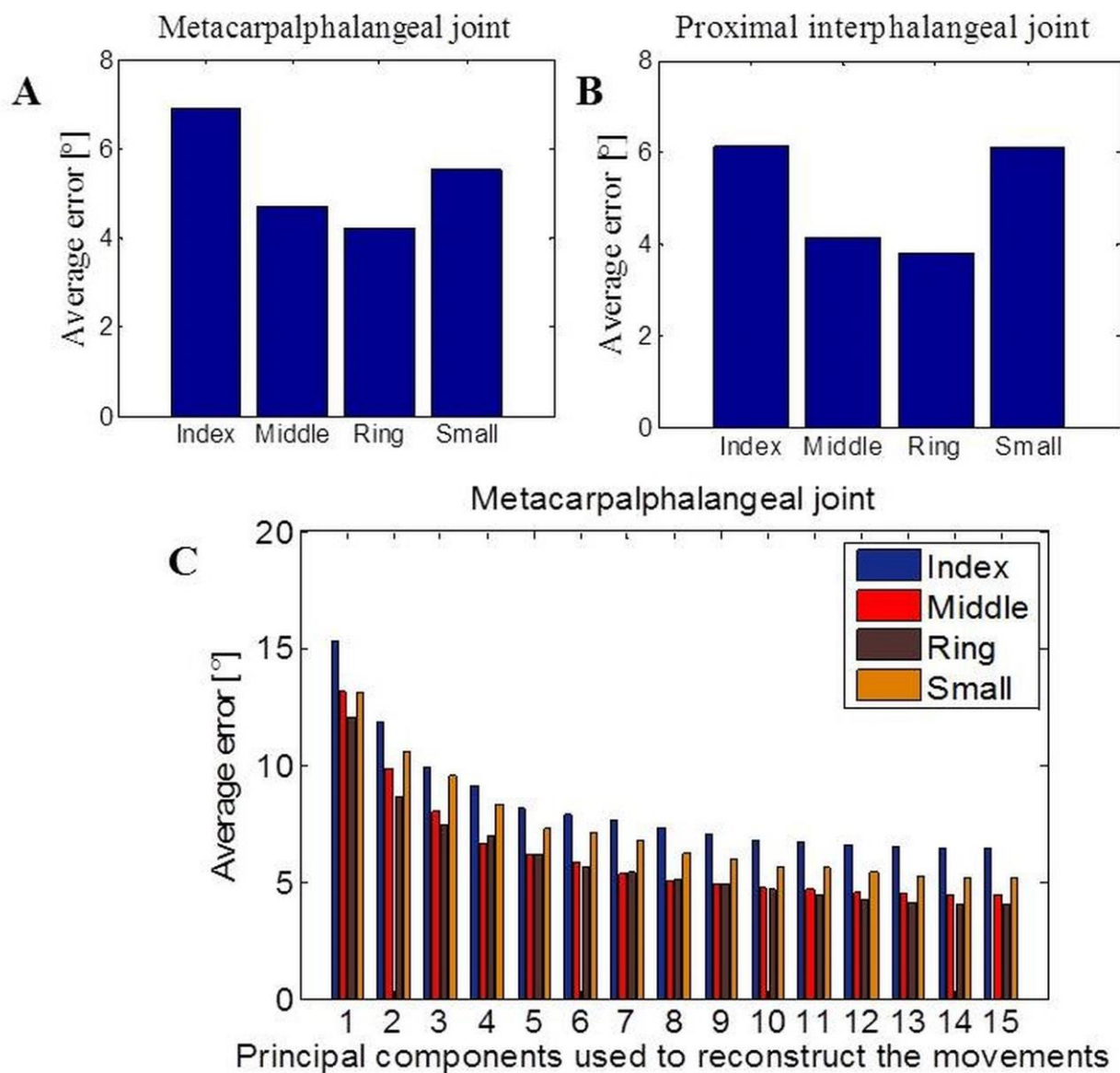
685

686

687

688

689



690

691

692

693

694

695

696

697